Chin. J. Astron. Astrophys. Vol. 2 (2002), No. 6, 487–500
(http://www.chjaa.org or http://chjaa.bao.ac.cn)

Chinese Journal of
Astronomy and
Astrophysics

Inclination of Broad Line Region in Narrow Line and Broad Line Seyfert 1 Galaxies

Tian-Zhi Zhang and Xue-Bing Wu ⋆

Department of Astronomy, School of Physics, Peking University, Beijing 100871

Received 2002 June 21; accepted 2002 October 8

Abstract The sizes of the Broad Line Region (BLR) of some Seyfert 1 galaxies and nearby quasars can be determined by the reverberation mapping method. Combining with the observed FWHM of Hβ emission line and assuming that the motion of BLR clouds is virialized, the black hole masses of these objects have been estimated. However, this method strongly depends on the poorly-understood geometry and inclination of the BLR. On the other hand, a tight correlation between the black hole mass and the bulge velocity dispersion was recently found for both active and nearby inactive galaxies. This may provide another method, independent of the BLR geometry, for estimating the black hole mass. Using this method for estimating the black hole mass and combining with the measured BLR size and FWHM of Hβ emission line, we derived the BLR inclination angles for 20 Seyfert 1 galaxies under the assumption that the BLR is disk-like. The derived inclination angles agree well with those derived previously by fitting the UV continuum and Hβ emission line profiles. Adopting a relation between the FWHMs of [O III]λ5007 forbidden line and the stellar velocity dispersion, we also estimated the BLR inclinations for 50 narrow line Seyfert 1 galaxies (NLS1s). We found that the inclinations of broad Line Seyfert 1 galaxies (BLS1s) are systematically greater than those of NLS1s, which seldom exceed 30°. This may be an important factor that leads to the differences between NLS1s and BLS1s if the BLR of NLS1s is really disk-like.

Key words: galaxies: active — galaxies: nuclei — galaxies: Seyfert

1 INTRODUCTION

Broad emission lines are prominent characters of active galactic nuclei (AGNs). These lines are generally believed to be produced in a broad line region (BLR) where gas is contained in many clouds and photoionized by the central extreme ultraviolet radiation. The emission line profiles are significantly broadened by bulk motions of the clouds. However, beyond this there is no general agreement on the physical conditions, geometry and kinematics of the BLR (see Netzer 1990 for a review).

⋆ E-mail: wuxb@bac.pku.edu.cn

BLR is not spatially resolved, therefore all the available information about its geometry was obtained from analyses of the variations of emission lines. A major tool for studying BLR is reverberation mapping (Blandford & Mckee 1982; Netzer & Peterson 1997). In this technique, time delay between the variations of the continuum and broad emission line flux is interpreted as the light travel time from the central region of AGN to the BLR. This provides an estimation of the radial size of BLR. So far the sizes of the BLRs of about three dozen Seyfert 1 galaxies and nearby quasars have been derived from this method. Wandel et al. (1999) and Ho (1999) compiled 20 Seyfert 1 galaxies with reliable BLR sizes obtained by reverberation mapping. Kaspi et al. (2000) after completing a 7.5 year monitoring observation, published the BLR sizes of 17 nearby quasars from the Palomar-Green quasar sample (Boroson & Green 1992). If in the BLR the dominating force is the gravitation of the central black hole, the kinematics of the BLR clouds can be regarded as virialized ($M \approx G^{-1}V^2R$). This assumption was discussed and justified by Peterson & Wandel (1999, 2000) for some Seyfert 1 galaxies. Then by combining the radius of BLR and FWHM of Hβ emission line which indicates the characteristic velocity of BLR clouds, the black hole mass can be estimated for a number of AGNs.

However, so far we do not know clearly the distribution of clouds in the BLR, and this prevents us from estimating the black hole mass more accurately (Krolik 2001). Usually the FWHM of Hβ line is adopted to estimate the velocity of BLR clouds, but the FWHM of Hβ can only tell us the apparent velocity rather than the intrinsic velocity. If we assume that the distribution of clouds is spherical and that the orbit of every cloud is random, we can easily convert the apparent velocity to an equivalent intrinsic velocity by introducing a coefficient to the mass function (Netzer 1990). However, if the actual distribution is not spherical but something anisotropic, such as a disk, the difference between the apparent and the intrinsic velocity will be determined by the inclination of the disk. In this case, the black hole mass derived from a spherical assumption will have to be corrected. This is very important for the estimation of black hole mass using the reverberation mapping technique (Mclure & Dunlop 2001; Wu & Han 2001).

Another reason for our concern with disk-like BLRs is that they may be related with the properties of NLS1s (Narrow Line Seyfert 1 Galaxies). NLS1 is a subclass of AGNs identified by Osterbrock & Pogge (1985), which have almost all properties of the Seyfert 1 nuclei but the Balmer emission lines are significantly narrower ($< 2000\,\mathrm{km\,s^{-1}}$). As a class they also have some other peculiar properties, such as strong optical FeII emission lines, strong soft X-ray excess and high-amplitude X-ray variability (Boller et al. 1996). The nature of NLS1 aside, we may simply imagine that a disk-like BLR is an intrinsically normal Seyfert 1 galaxy that has narrower emission lines at low inclination angle. Then an interesting question arises: Are NLS1s just normal Seyfert 1s at lower BLR inclinations? Or are only some NLS1s normal Seyfert 1s at lower inclinations while some others are really physically different? The study of BLR inclinations of NLS1s will be very helpful to answer these questions.

We will discuss the possibility and evidence of a disk-like BLR in the next section. In Section 3 we will show our method of estimating the BLR inclinations and give a detailed analysis of the reliability of the method. A discussion on the results will appear in Section 4.

2 POSSIBILITY OF A DISK-LIKE BLR

The broad emission lines of AGNs are believed to be emitted from the broad line region which is about 0.1 to 1pc far away from the center of the AGN. Unfortunately there are no generally accepted theoretical models or observations that can tell us what the geometry of a BLR really is. Reverberation mapping can only be used to measure the size of the BLR but nothing about its configuration. The geometrical disposition and the pressure of the gas are ultimately determined by the history of forces acting upon it but we know little about this history for sure (Krolik 1999). A hopeful way to study the BLR configuration is to analyze the emission line profiles, since the line broadening is due to the velocity dispersion of the emitting gas. For a few AGNs there was an accurate determination of the disk geometry possible by modeling the asymmetries of very broad (FWHM $> 12\,000$ km s^{-1}) double-peaked emission line profiles (Rokaki & Boisson 1999 and reference in). However, the observations show a significant diversity in the shape and width of broad emission line profiles among different AGNs, which implies that some fundamental dynamical parameters vary significantly among the AGN population, or that the BLR undergoes secular evolution (Robinson 1995). Therefore, we will not attempt a final word on the geometry of BLR here. It is better to compare different assumptions with the observations and find out the most suitable one, since we often have to take assumptions.

There are two major options for the configuration of BLR at present — disk-like BLR and sphere-like BLR. Though recently a jet-like BLR with biconical configuration is implied by the finding of blue wings in UV emission lines, namely, Lyα and C IV λ1549, with line widths amounting to 5000 km s^{-1} in some NLS1s (Rodríguez-Pascual et al. 1997), these NLS1s have narrower optical BLR emission lines (e.g., Hα, Hβ) whose FWHMs are about 1000 km s^{-1}. It seems that these optical emission lines may not be produced in the same region as the UV emission lines. Therefore, we will only compare the disk-like and sphere-like assumptions for BLR configuration.

An obvious evidence supporting the disk-like BLR model is that for quasars there is a highly significant correlation between the line widths (FWHM) of broad Hβ lines and R, the ratio of radio core flux density to the extended radio lobe flux density (Wills & Browne 1986). Among the objects with higher R, there is clear absence of objects with broader emission lines. In the relativistic beaming model for radio sources, R is related to the angle between the radio axis and the line of sight. In other words, this correlation means that the widths of emission lines are broader when the inclination angle is higher. Then, if the relativistic beaming model is correct, this correlation will be consistent with the motion of the emission line gas being confined predominantly to a plane perpendicular to the radio axis. Another evidence is from observations of radio galaxies. Antonucci (1984) found that optical polarizations of quiescent quasars are all or nearly all aligned with the associated radio structure axes. Polarizations of Seyfert 1 galaxies tend to aligned with the radio axes, while those of Seyfert 2 galaxies are perpendicular to the radio axes. Among radio galaxies there is a significant excess of parallel objects. This indicates an axial symmetry for the broad line region. From these two lines of evidence, it seems that spherical symmetry may not be realistic for the BLRs in quasars and radio galaxies.

In principle we can also study the accuracy of the disk-like assumption with statistics. If the intrinsic velocity of the BLR clouds have a typical distribution, such as a Gaussian form, for the sphere-like BLR the clouds' orbits are random, then the FWHM of Hβ emission lines which indicates the apparent velocity, will also have a Gaussian distribution, but the variance is broader. However, for the disk-like BLR, if its three spatial rotation angles are random, the possibility of observing an object with inclination angle θ is proportional to $\sin\theta$ and $P(0 < \theta < i) = 1 - \cos i$. Therefore, an object with a higher inclination angle is more likely to be observed than one with a lower inclination angle. Then the observed FWHM distribution of Hβ lines will not be Gaussian but will be biased toward high inclination angles and will have a broader variation. Theoretically, we can test the disk-like assumption by studying the FWHM distribution of Hβ emission lines, but, in practice it is difficult if not impossible. First, how to select the sample is a problem. If we examine the distribution of line widths, we must select the sample by some criteria independent of line widths. However, there are many correlations between line widths and other quantities. We must take care to avoid biases. More difficult is that we do not know the intrinsic distribution of line widths for we do not know clearly the kinematics of BLR. It may be Gaussian, random or something else. If the central engines in different class AGNs are varied, there may be no uniform distribution at all. Therefore, if someone wants to do this he will have to make an assumption on the intrinsic velocity distribution of the BLR clouds, such as what McLure & Dunlop (2001, 2002) did in their recent studies. One can use this method to calculate something but it is not advisable to test an assumption by introducing new assumptions, at least not in this circumstance.

Maybe a more reliable method to test the disk-like BLR assumption is to calculate results under this assumption and compare the results with those derived from other independent method.

3 CALCULATION OF INCLINATION ANGLE OF BLR

3.1 The Method

The method we will use in this paper has been described by Wu & Han (2001), but it still needs to be investigated in more detail. As we mentioned previously, if the dominant force in the BLR is the gravitation of the central black hole, the motion of BLR clouds will be virialized and the clouds will orbit the black hole with Keplerian velocities. Then the central black hole mass is given by $M = G^{-1}V^2R$, where V is the velocity of the clouds and R is the radius of the BLR which can be obtained by the reverberation mapping method. If we also know the velocity V, we can estimate the black hole mass. It is generally believed that the emission line widths indicate the cloud velocities, so the next problem is how to convert the FWHM of Hβ to V. In the sphere-like BLR model the orbits of clouds are random and $V = \sqrt{3}/2V_{\rm FWHM}$, where $V_{\rm FWHM}$ is the FWHM of Hβ line, the factor $\sqrt{3}/2$ is to account for velocities in three dimensions and for using half of the FWHM (Kaspi et al. 2000). In the disk-like BLR model, the $V_{\rm FWHM}$ is generally given as (Wills & Browne 1986):

$$V_{\rm FWHM} = 2(V_{\rm r}^2 + V_{\rm p}^2 \sin^2\theta)^{1/2}\,, \tag{1}$$

here θ is the angle between the line of sight and the axis of the disk, $V_{\rm p}$ is the component in the plane of the disk, and $V_{\rm r}$ is a random isotropic component. Usually $V_{\rm r}$ is believed to be significantly smaller than $V_{\rm p}$. Then, ignoring $V_{\rm r}$ (we will discuss its effect on the results in Section 3.2), the mass of the central black hole can be given as:

$$M_{\rm rev} = \frac{V_{\rm FWHM}^2 R}{4\sin^2\theta G}, \tag{2}$$

where $M_{\rm rev}$ is the black hole mass derived by considering the inclination of BLR. It is clear that the inclination plays an important role in determining the black hole mass; however, usually we do not have any information on the inclination angle of the AGN.

Before further discussion, let us take a look at the relationship between the $M_{\rm rev}$ derived from the two different models. In the sphere-like BLR model, we have

$$M_{\rm rev} = \frac{3V^2_{\rm FWHM}R}{4G}\,. \tag{3}$$

Comparing Eq. (3) with Eq. (2) we can find that the black hole mass derived from the sphere-like BLR model is equivalent to the black hole mass derived from the disk-like BLR when $\sin\theta = \sqrt{3}/3$, or $\theta = 35^\circ$. In the uniform model of Seyfert 1s and Seyfert 2s (Antonucci & Miller 1985), Seyfert 1s and Seyfert 2s differ because of the viewing angle and the angle 35° is approximately the critical angle of Seyfert 1s. Therefore, the black hole masses derived from the sphere-like BLR model will, on average, be smaller than from the disk-like BLR model, since there must be many Seyfert 1s with viewing angles smaller than the critical angle.

The reverberation mapping method is not the only method for deriving the black hole mass. Recently, Gebhardt et al. (2000) and Ferrarese & Merritt (2000) reported a strong relationship between the black hole mass $M_\bullet$, and the stellar velocity dispersion σ_e, for nearby galaxies. The relation is expressed as (Gebhardt et al. 2000):

$$M_\bullet = 1.2\times10^8 M_\odot\left(\frac{\sigma_e}{200\,{\rm km\,s^{-1}}}\right)^{3.75}. \tag{4}$$

$M_\bullet$ was determined from stellar or gas kinematics and σ was obtained for a large aperture extending to the galaxy's effective radius, thus insensitive to the influence of the black hole. More recent studies indicated that some Seyfert galaxies also follow the same $M_\bullet$-σ relation (Ferrarese et al. 2001). Nelson (2000) examined this relation for AGNs with black hole masses derived from the reverberation mapping method, adopting the stellar velocity dispersion values derived from the FWHMs of [O III] λ5007 line based on a relation σ = FWHM ([O III])/2.35 (Nelson & Whittle 1996). He found that the $M_\bullet$-σ relation for the AGN sample is very similar to that for nearby galaxies; however, for the AGN sample there is a little change of the relation to smaller black hole masses for a given velocity dispersion σ_*, and it is more scattered. There may be some other explanations for these differences. However, as we mentioned above, the black hole mass derived in a sphere-like BLR model will be, on average, smaller than that in a disk-like BLR model. If the disk-like BLR model is correct, the black hole masses derived for the sphere-like BLR model would be too small and a larger scatter would be very natural.

In the present paper we assume that the relation of the black hole mass and the stellar velocity dispersion is exactly the same for normal galaxies and AGNs, that any difference is only due to a bad assumption – the sphere-like BLR. Extending Eq. (4) to AGNs, we can derive the black hole mass from the stellar velocity dispersion. The most important advantage of such a method is that it is independent of the BLR geometry. Then from Eq. (2) we can determine the inclination angle of the disk-like BLR from:

$$\sin\theta = \frac{V_{\rm FWHM}}{2}\times\sqrt{\frac{R}{M_\sigma G}}, \tag{5}$$

where M_σ is the black hole mass derived directly from the velocity dispersion σ_*.

3.2 The Reliability of the Method

In our method of calculation we have made certain assumptions with their attendant uncertainties. Therefore, we must demonstrate the reliability of our method before giving our results.

First, we assumed that the motion of BLR clouds is virialized. This assumption is the basis of the measurement of black hole mass by the reverberation mapping method, and it has been extensively discussed and verified by some authors, e.g., Peterson & Wandel (1999, 2000). It is known that the BLR may be stratified, with different emission lines emitting from different distances from the central source. Typically, different lines have different widths. Then if the motion of the BLR clouds is Keplerian, the black hole masses derived from different emission lines will be the same. With many analyses, Peterson & Wandel (1999, 2000) derived a result supporting the virial assumption. For our work, we think it is better to estimate the effect of non-virial motions on our results. If the motion of the BLR clouds is not merely virial but contains inflow or outflow, the variable $V_{\rm FWHM}$ should be changed to $\sqrt{V_{\rm FWHM}^2 - 4V_{\rm r}^2}$ in Eq. (5). Then Eq. (5) will be changed to:

$$\sin\theta = \frac{\sqrt{V_{\rm FWHM}^2 - 4V_{\rm r}^2}}{2} \times \sqrt{\frac{R}{M_\sigma G}}. \tag{6}$$

It is difficult to measure the value of $V_{\rm r}$, but we can make a rough estimation. If the disk-like BLR model is correct, the object that has a zero inclination angle will have a zero line width. In the sample of 20 Seyfert 1 galaxies with BLR sizes measured by reverberation mapping, the smallest measured FWHM of $H\beta$ is the $1170\,{\rm km\ s^{-1}}$ belonging to NGC 4051. If we suppose that NGC 4051 has a zero inclination angle and the line width is from $V_{\rm r}$, then we can derive an approximate $V_{\rm r} = 500\,{\rm km\ s^{-1}}$. If the intrinsic velocity of BLR clouds in different AGNs are approximately the same (though they may have a certain spread), then different AGNs should have approximately the values of $\sqrt{R/M_\sigma G}$. Then we check that the object NGC 5548, which has a second largest FWHM of $H\beta$ line among the 20 Seyfert 1 galaxies, has an inclination angle of 90°, combining with $V_{\rm r}$ we can give approximately $\sqrt{R/M_\sigma G} = 0.0003$. Therefore, for an object with a real inclination angle θ we obtain an estimated inclination angle when ignoring $V_{\rm r}$. The result is shown in Fig. 1, where θ is the intrinsic angle and θ' is the estimated angle.

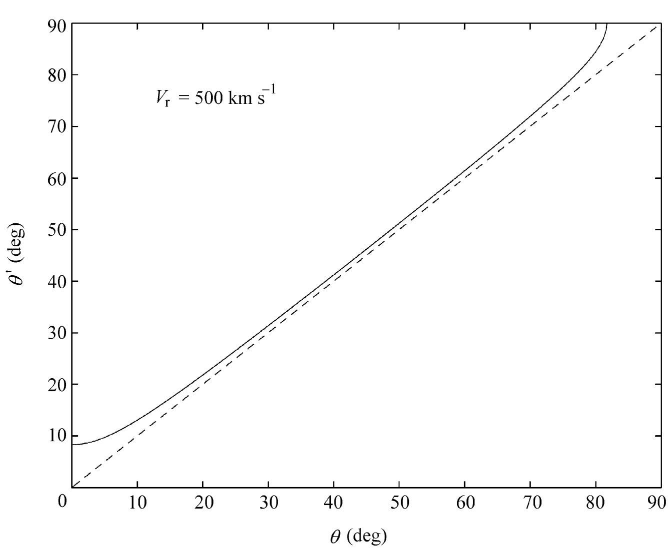

Fig. 1 Solid curve is the relation between the intrinsic angle θ and the calculated angle θ' for $V_{\rm r} = 500\,{\rm km\,s^{-1}}$. The dash line is the reference line $\theta' = \theta$.

In this figure we can see that the effect of ignoring V_r on the results is only significant when the angle is smaller than 10° or greater than 80°, that for intermediate angles the error is less than ten percent. Therefore, we can derive a reliable inclination angle even when the real motion of BLR clouds has a significant deviation ($V_r = 1/7V_p$) from Keplerian motion. Note that in this rough estimation we assumed that all AGNs in our sample have the same intrinsic BLR cloud velocity, but the dispersion may be larger in practice. Even though there is a slight effect on the error estimation of V_r, it has nearly no effect on our inclination angle.

Secondly, we assumed that AGNs have the same relation between the black hole mass and the velocity dispersion as normal galaxies. Though there exists such a relation Eq. (4), its meaning is largely statistical. Moreover, there are only a few Seyfert 1 galaxies with available velocity dispersion data. For others the velocity dispersion values were converted from the FWHM of [O III] $\lambda\,5007$ line, which involved another uncertainty. All these uncertainties impact on the estimated black hole mass M_σ. However, it is difficult to evaluate these uncertainties in individual cases: we can only estimate a reasonable error for all the objects and see whether it will lead to unreasonable results.

In their paper, Gebhardt et al. (2000) gave a measured scatter of 0.30 dex in their black hole mass in Eq. (4) at a fixed dispersion. Given the likely measurement errors, they thought that the intrinsic scatter is probably < 0.15 dex. Combining the potential error of FWHM of [O III] $\lambda\,5007$ line, we estimate an error of 100 percent is a reasonable maximal estimation for M_σ. Then assuming an intrinsic black hole mass M and an inclination angle θ, let us see what results Eq. (6) will lead to when the calculated black hole mass M' is $2M$ and $1/2M$, respectively. The results are shown in Fig. 2. We can see that the error is acceptable when the angle is smaller than 40°, but it grows rapidly with increasing inclination angle: when $\theta > 50°$ the results are completely uncertain. However, according to the unified model of AGNs, Seyfert 1s are AGNs

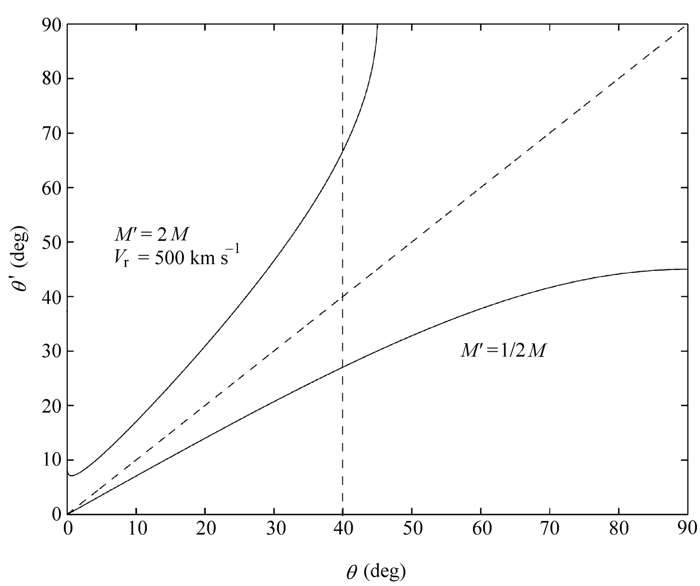

Fig. 2 The $\theta \sim \theta'$ relation for taking twice the intrinsic black hole mass (upper) and half the intrinsic mass (lower).

at a low inclination angle and a credible critical angle is 40°. Then, the probability of encountering a Seyfert 1 at a large inclination angle is small. There is another variable R, which may lead to errors in the same way as does M_σ, but as its error was much smaller than that of M_σ (20–30% on average), it was ignored. Note that what we do here is not error analysis, but reliability analysis. The main uncertainties of our method are given their maximum values, they may be not so large in practice. We only want to show that even if we allow maximum uncertainties, our method will not give totally unreasonable results.

3.3 BLR Inclinations of BLS1s and NLS1s

We collected 20 Seyfert 1 galaxies with BLR sizes derived by reverberation mapping, 11 of them have measured stellar velocity dispersions and their BLR inclinations have been estimated in Wu & Han (2001). For the rest nine objects, we estimated their stellar velocity dispersions from the FWHMs of [O III]λ 5007 emission line (Nelson & Whittle 1995). The BLR sizes and FWHMs of Hβ and [O III] λ5007 lines for these 20 Seyfert 1 galaxies were compiled by Nelson (2000). From Eqs. (4) and (5) we can estimate the black hole masses and BLR inclinations for these objects. The results are summarized in Table 1. Note that we are unable to derive the inclination for 3C 390.3 because its FWHM of Hβ is too large, leading to an unreasonable value of $\sin\theta$. One possibility for the failure of our method in this case may be that the BLR structure of this kind of radio-loud objects is probably quite different from other radio-quiet Seyfert 1s.

Table 1 BLR Inclination Angles for 20 BLS1s

Name	R (BLR)	FWHM (Hβ)	ΔFWHM(Hβ)	FWHM(Hβ)	σ	FWHM ([O III])	Γ	M_σ (BH)	θ	θ
		rms	rms	mean			Rosat		rms	mean
	light day	km s^{-1}	km s^{-1}	km s^{-1}	km s^{-1}	km s^{-1}		$10^7 M_\odot$	deg	deg
3C 120	42	2210	120	1910	162	230	2.15	5.45	25	22
NGC 4051	6.5	1230	60	1170	80	190	2.58	0.39	21	20
NGC 4151	3	5230	920	5910	93	425	2.06	0.68	50	60
NGC 4593	4	···	···	3720	124	255	2.08	2.00	···	22
NGC 5548	21.2	5500	400	6300	183	410	2.3	8.60	37	44
Mrk 590	20	2170	120	2470	169	400	2.41	6.38	16	18
Mrk 817	15	4010	180	4490	142	330	2.9	3.32	37	42
NGC 3227	10.9	5530	490	4920	144	485	1.19	3.50	43	37
NGC 3516	7	···	···	4760	124	250	2.15	2.00	···	38
Mrk 110	18.8	1670	120	1430	86	290	2.4	0.51	45	37
Mrk 79	17.7	6280	850	4470	130	350	2.57	2.39	···	58
3C 390.3	22.9	10500	800	10000	···	410	1.86	7.12	···	···
Akn 120	37.4	5850	480	5800	···	490	2.61	13.90	42	42
F9	16.3	5900	650	5780	···	425	2.42	8.25	35	35
IC 4329A	1.4	5960	2070	5050	···	550	1.71	21.6	6	5
Mrk 279	10	···	···	5360	···	580	2.15	26.1	···	13
Mrk 335	16.4	1260	120	1620	···	280	2.92	1.71	15	20
Mrk 509	76.7	2860	120	2270	···	520	2.58	17.45	24	19
NGC 3783	4.5	4100	1160	3790	···	230	2.45	0.83	41	38
NGC 7469	4.9	3220	1580	3000	···	360	2.38	4.40	13	13

Two columns of angle correspond to two columns of FWHM of [O III]λ5007 which are derived from rms and mean statistical method separately.

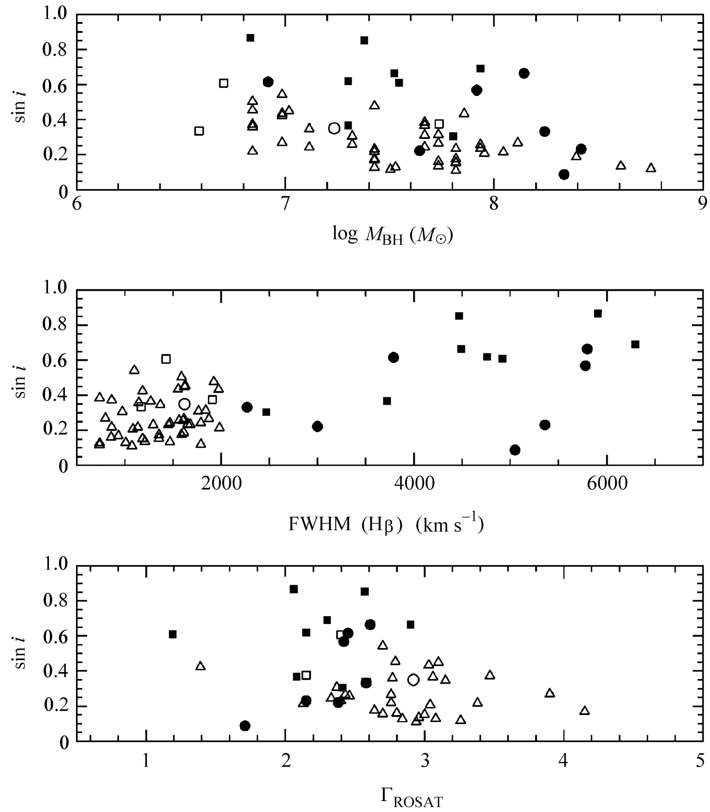

Fig. 3 Derived BLR inclinations of BLS1s (solid symbols) and NLS1s (open symbols) plotted against black hole mass, apparent Hβ velocity and X-ray photon index. Objects with black hole masses derived from measured central velocity dispersions are shown as squares; from [OIII] λ5007 velocities, as triangles.

Recently Véron et al. (2001) carefully measured the emission line properties of about 60 NLS1s. The FWHMs of the Hβ and [OIII] λ5007 lines were obtained for 50 NLS1s. Therefore, we estimate the black hole mass for these 50 NLS1s by deriving the central velocity dispersions from the FWHMs of [OIII] λ5007 line (Nelson & Whittle 1995). Using the empirical method of Kaspi et al. (1999), we can also estimate the BLR size of these NLS1s from their optical luminosities (Wang & Lu 2001). Their apparent Hβ velocities have been measured by Véron et al. (2001). Adopting the same method as we described above, we can derive the BLR inclinations of these NLS1s. Note that for several NLS1s, the measured velocities of [OIII] λ5007 line are smaller than 200 km s^{-1}, which corresponds to the 3.4Å FWHM resolution of detector used by Véron et al. (2001). These small values of FWHM of [OIII] λ5007 line are quite uncertain and therefore we did not derive the black hole masses for these objects. On the other hand, we also did not give estimations of black hole masses for several NLS1s with extremely high (> 800 km s^{-1}) FWHM values of the [OIII] λ5007 line because most of these objects are radio loud. The results are summarized in Table 2.

Table 2 BLR Inclination Angles for 50 NLS1s

Name	Γ	$\Delta\Gamma$	FWHM (Hβ) km s^{-1}	FWHM ([O III]) km s^{-1}	R (BLR) light day	M (BH) $10^7 M_\odot$	θ deg
Mark 335	3.1	0.05	1620	245	16.4	1.04	27
TonS 180	3.04	0.01	1085	435	89.8	8.98	14
Mark 359	2.4	0.1	900	180	19	0.33	29
MS 01442–0055	2.7	0.2	1100	240	63.7	0.97	39
Mark 1044	3.08	0.09	1010	335	15	3.37	9
HS 0328+0528	···	···	1590	220	18.9	0.7	35
IRAS 04312+4008	2.8	0.6	860	380	52.2	5.41	11
IRAS 04416+1215	2.96	0.5	1470	650	92.8	40.48	9
IRAS 04576+0912	···	···	1210	380	18.5	5.41	1
IRAS 05262+4432	···	···	740	365	342.3	4.65	26
RXJ 07527+2617	3	0.26	1185	400	29.9	6.55	10
Mark 382	3.09	0.23	1280	155	23	0.19	82
Mark 705	2.33	0.09	1790	365	23.6	4.65	16
Mark 707	2.4	0	1295	315	23.2	2.68	15
Mark 124	···	···	1840	380	43	5.41	21
Mark 1239	2.94	0.14	1075	400	18.9	6.55	7
IRAS 09571+8435	1.39	0.4	1185	240	33.4	0.97	29
PG 1011–040	···	···	1455	400	46.3	6.55	16
PG 1016+336	···	···	1590	315	8.9	2.68	12
Mark 142	3.15	0.11	1370	260	22.7	1.3	24
KUG 1031+398	4.15	0.1	935	315	23.6	2.68	11
RXJ 10407+3300	2.13	0.15	1985	460	35.3	11.07	14
Mark 734	3.63	0.19	1825	180	59.6	0.33	···
Mark 739E	2.43	0.14	1615	380	39.9	5.41	17
MCG 06.26.012	2.77	0.08	1145	220	18.6	0.7	24
Mark 42	2.76	0.23	865	220	12.4	0.7	14
NGC 4051	2.84	0.04	1120	200	6.5	0.49	17
PG 1211+143	3.03	0.15	1975	410	101	7.19	31
Mark 766	2.79	0.11	1630	220	14.8	0.7	32
MS 12170+0700	···	···	1765	365	39.4	4.65	21
MS 12235+2522	3.9	0.3	800	240	29.9	0.97	18
PG 1244+026	3.26	0.13	740	330	21.2	3.19	8
NGC 4748	2.46	0.15	1565	295	15.5	2.09	17
Mark 783	···	···	1655	430	47.4	8.6	16
R14.01	···	···	1605	430	60.5	8.6	17
Mark 69	···	···	1925	315	44.9	2.68	33
Mark 478	3.06	0.03	1270	365	105.3	4.65	25
PG 1448+273	3.17	0.32	1050	155	69.1	0.19	···
Mark 486	···	···	1680	400	34.9	6.55	16
Mark 493	2.84	0.14	740	315	21.7	2.68	8
EX O16524+3930	2.7	0.2	1355	400	24	6.55	10
B31702+457	2.37	0.18	975	295	56.4	2.09	21
RXJ 17450+4802	2.64	0.13	1355	400	30.2	6.55	12
Kaz 163	2.76	0.03	1875	480	71.7	12.99	18
HS 1817+5342	···	···	1615	570	91.2	24.74	13
HS 1831+5338	···	···	1555	240	20.7	0.97	30
Mark 896	3.38	0.05	1135	315	27.1	2.68	15
Akn 564	3.47	0.07	865	220	35.4	0.7	26
HS 2247+1044	···	···	1790	710	69.6	56.37	8
Kaz 320	···	···	1470	260	9.5	1.3	16

In Figure 3 we plot the derived $\sin i$ values for both BLS1s and NLS1s against their black hole masses, observed Hβ FWHMs and X-ray photon indices. If the black hole mass can be estimated by the FWHMs of [OIII] λ5007 line, we see that the black hole masses of NLS1s are comparable to those of BLS1s. This is contrary to some previous claims that the black hole masses of NLS1s are significantly smaller than those of BLS1s (Mathur et al. 2001; Wang & Lu 2001). Our result, however, is probably consistent with the recent finding that the properties of narrow emission line region are almost the same for both BLS1s and NLS1s (Nagao et al. 2001). From Figure 3 we can clearly see that the derived inclinations of BLR for NLS1s are systematically smaller than those for BLS1s. The BLR inclinations of most NLS1s are smaller than 30°, while those of most BLS1s lie in the range of 20°to 60°(see also Wu & Han 2001). This may indicate that the BLR inclinations of NLS1s are significantly smaller than those of BLS1s. Indeed, some theoretical ideas inferred from the X-ray observations of NLS1s have suggested that NLS1s may be systems viewed face-on. (Boller et al. 1996; Puchnarewicz et al. 1992). The smaller BLR inclinations can also satisfactorily explain the relative narrower Hβ lines in observed NLS1s if their BLRs are disk-like. A positive correlation between $\sin i$ and FWHMs of Hβ line can be clearly observed for both NLS1s and BLS1s in the middle panel of Figure 3. In addition, Figure 3 shows that there is also a negative correlation between $\sin i$ and the X-ray photon index. This is expected because the observed FWHMs of Hβ line are closely related to the X-ray photon index (Boller et al. 1996).

4 DISCUSSION

4.1 An Independent Check of Our Results

Though we derived the BLR inclination angle of both broad line and narrow line Seyfert 1s, we would like to mention that the disk-like BLR is still an assumption. In order to check our results we must compare them with those obtained by some independent methods. Fitting the profiles of broad emission lines is another possible method to derive the BLR inclination, since characteristic asymmetries in the apparent line profiles depend on the orientation of the BLR. However, as we mentioned above, only for a few objects with extremely larger FWHMs (FWHM $> 12\,000\,\mathrm{km\,s^{-1}}$) has the BLR geometry been so assessed. For objects where the BLR clouds have lower Keplerian velocities, the line profiles are not significantly asymmetric, and the inclination angle cannot be determined accurately. In order to increase the precision of estimating the black hole and disk parameters, Rokaki & Boisson (1999) fitted the UV continuum, the broad Balmer line fluxes and the line profiles consistently for a carefully selected sample of AGNs, with the effects of general relativity taken into consideration. They showed that a consistent line and continuum fitting gives a unique solution for estimating the black hole mass and the inclination angle of the disk.

We compared our estimated inclination angles for nine objects in common with Rokaki & Boisson (1999). The results obtained by them and us are remarkably consistent. Except two objects that have relatively larger differences ($\approx 20°$), all the others have differences less than 10°. The comparison is shown in Fig. 4. Note that there are two groups of inclination angles in Rokaki & Boisson's results, fitted for Schwarzschild black hole and Kerr black hole respectively. The comparison above is for the former case, the inclination angles estimated by Rokaki & Boisson (1999) for the later case are on average systematically smaller than ours, but they still have a significant correlation with ours.

The inclination angles derived by them and by us were based on very different methods, one on the UV continuum and the Hβ profile, the other on the FWHM of Hβ line, the radius of BLR from reverberation mapping and the stellar velocity dispersion or the FWHM of [OIII] λ5007. The agreement between them and us, if not by chance, would be an indication of the self-consistency of the essential assumption of a disk-like BLR in AGNs. From the list of inclination angles in our sample 1, we note that there is only one object for which we did not derive this angle ($\sin\theta > 1$), for all others the largest angle is 60° and most of the angles are smaller than 40°; this is consistent with the unified model of AGN.

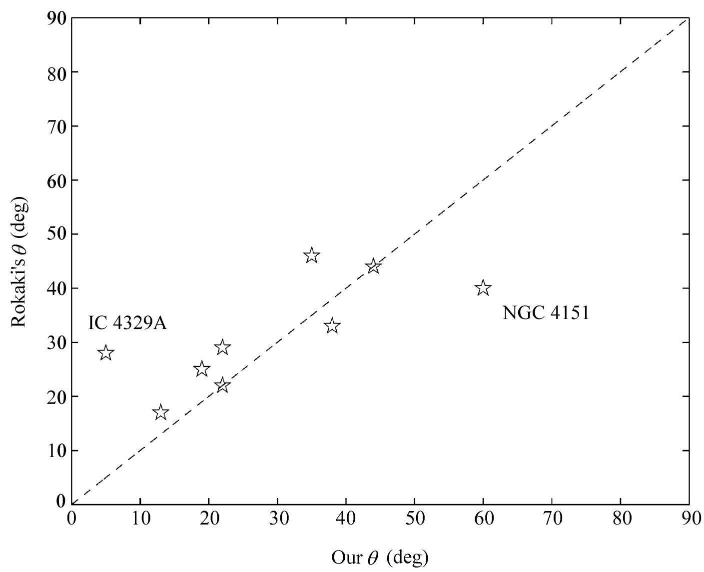

Fig. 4 A plot of the BLR inclination angles derived by us and by Rokaki & Boisson (1999). The dash line marks exact equality.

Our results support the possibility that the NLS1s are objects with lower BLR inclinations and viewed nearly face-on if their BLR is of disk-like configuration. This has been inferred from their narrower emission line widths (Boller et al. 1996). Positive evidence for this scenario has been also given by Boller et al. (1997) to explain the persistent giant and rapid X-ray variability in the radio-quiet, ultrasoft, strong Fe II, narrow-line Seyfert 1 galaxy IRAS 13224–3809. They suggested that the relativistic boosting effects may be relevant to understanding the strong X-ray variability of some X-ray steep-spectrum Seyfert galaxies more generally. Therefore, our results seem to be consistent with these previous arguments. However, we must keep in mind that the physics of both the BLR and NLR of AGNs is not well understood at present. NLS1s are also likely to be intrinsically different objects from BLS1s. More observations and theoretical efforts are still needed before a clearer conclusion is reached.

4.2 The Uncertainties of the Results

Although we have proved the reliability of our method in Section 3.2, more discussion should be made here because of the complexity of the problem. The problem is that our sample is not a uniform sample. There are three different classes of objects in our sample – BLS1s with measurements of σ, BLS1s without direct measurements of σ, but derived from the FWHM of [OIII] λ5007, and NLS1s without direct measurements of σ or the size of BLR.

For the first class, the BLS1s with measurements of σ, the average uncertainty of these objects is 10% and as we have discussed in Section 3.2, when this uncertainty is combined with the scatter in the $M_{\rm BH}$–σ relation (0.15 dex) and the uncertainty in the size of the BLR (R), we arrive at a total maximum uncertainty of a factor of two. For these objects our method works well. For the second class, BLS1s without direct measurements of σ, we use the correlation between σ and the FWHM of [O III] λ5007 to convert the measurements of the FWHM of [O III] λ5007 to σ (Nelson & Whittle 1996). This means an additional uncertainty. It is difficult to find out how large this uncertainty is, but Nelson (2000) has shown that the black hole masses in the central of AGNs derived from the reverberation mapping method, with the velocity dispersion converted from the FWHM of [O III] λ5007, agree well with the $M_{\rm BH}$–σ relation defined by nearby hot galaxies. This may convince us that the uncertainties of the σ derived from the width of [O III] λ5007 are not very large. The most uncertain class of objects is the NLS1s. For these objects, we did not have direct measurements of σ, and we also did not make direct measurements of the size of the BLR: we derived the BLR size using the empirical method of Kaspi et al. (1999). Though Kaspi's method is derived mainly from the statistics of BLS1s, and there is no proof that the relation is valid for NLS1s, several NLS1s with direct measurements of the size of the BLR did not prove the relation to be invalid for NLS1s. But this will lead to another uncertainty in the results derived from these objects.

In sum, of the three classes of objects, the most accurate inclination angles are derived from the BLS1s with measurements of σ, and we can estimate their uncertainties. The least results are derived from the sample of NLS1s and we do not even know how large their uncertainties are. However, all the difficulties mainly come from the fact that we do not have enough observational data rather than from the method itself. In the future, when we have more observations on these objects we shall be able to derive more accurate results.

Acknowledgements We thank Professors J. L. Han and J. Y. Wei for many useful discussions. This work is partially supported by the NSFC (No. 10173001) and by the Scientific Foundation for Returned Overseas Chinese Scholars, Ministry of Education, China.

References

Antonucci R. R. J., 1984, ApJ, 278, 499
Antonucci R. R. J., Miller J. S., 1985, ApJ, 297, 621
Blandford R. D., McKee C. F., 1982, ApJ, 255, 419
Boller T., Brandt W. N., Fink H., 1996, A&A, 305, 53
Boller T., Brandt W. N., Fabian A. C., Fink H. H., 1997, MNRAS, 289, 393
Boroson T. A., Green R. F., 1992, ApJS, 80, 109
Ferrarese L., Merritt D., 2000, ApJ, 539, L9
Ferrarese L., Pogge R. W., Peterson B. M., Merritt D., Wandel A., Joseph C. L., 2001, ApJ, 555, L79
Gebhardt K., Bender B., Bower G. et al., 2000, ApJ, 539, L13
Ho L., 1999, In: S. Charkrabarti, ed., Observational Evidence for the Black Holes in the Universe, p.157
Kaspi S., Netzer H., 1999, ApJ, 524, 71
Kaspi S., Smith P. S., Netzer H., Maoz D., Jannuzi B. T., Giveon U., 2000, ApJ, 533, 631
Krolik J. H., 1999, Active Galactic Nuclei, Princeton University Press, p.323
Krolik J. H., 2001, ApJ, 551, 72
Mathur S., Kuraszkiewicz J., Czerny B., 2001, New Astronomy, 6, 321

McLure R. J., Dunlop J. S., 2001, MNRAS, 327, 199
McLure R. J., Dunlop J. S., 2002, MNRAS, 331, 795
Nagao T., Murayama T., Taniguchi Y., 2001, ApJ, 546, 744
Netzer H., 1990, In: T. J.-L. Courvoisier, M. Mayor, eds., Active Galactic Nuclei, Berlin: Springer-Verlag, p.57
Nelson C. H., 2000, ApJ, 544, L91
Nelson C., Whittle M., 1995, ApJS, 99, 67
Nelson C., Whittle M., 1996, ApJ, 456, 96
Netzer H., Peterson B. M., 1997, In: D. Maoz, A. Strenberg, E. M. Leibowitz, eds., Astronomy Time Series, Dordrecht: Kluwer, p.85
Osterbrock D. E., Pogge R. W., 1985, ApJ, 297, 166
Peterson B. M., Wandel A., 1999, ApJ, 521, L95
Peterson B. M., Wandel A., 2000, ApJ, 540, L13
Puchnarewicz E. M., Mason K. O., Cordova F. A. et al., 1992, MNRAS, 256, 589
Robinson A., 1995, MNRAS, 272, 647
Rodríguez-Pascual P., Mas-Hesse J. M., Santos-Lleó M., 1997, A&A, 327, 72
Rokaki E., Boisson C., 1999, MNRAS, 307, 41
Véron-Cetty M.-P., Véron P., Gonçalves A. C., 2001, A&A, 372, 730
Wandel A., Peterson B. M., Malkan M. A., 1999, ApJ, 526, 579
Wang T., Lu Y., 2001, A&A, 377, 52
Wills B. J., Browne I. W. A., 1986, ApJ, 302, 56
Wu X.-B., Han J. L., 2001, ApJ, 561, L59